X26A Hard X-Ray Microprobe

Antonio Lanzirotti, Steve Sutton
The University of Chicago
Consortium for Advanced Radiation Sources

Beamline Overview

•Beamline X26A at has been used as a synchrotron x-ray microprobe since 1986
•Remains the only dedicated hard x-ray microprobe available to users at the NSLS.
•Participating Research Team (PRT)
    •The University of Chicago's Consortium for Advanced Radiation Sources (CARS)
    •The University of Georgia's Savannah River Ecology Laboratory (SREL)
    •Brookhaven National Laboratory's Environmental Sciences Department.
• Core research mission of X26A remains in Earth and Environmental Sciences
    •speciation, transport, and reactions of chemical species in the Earth.
•X-ray microprobe techniques offer distinct advantages over other analytical techniques by allowing analyses to be done *in-situ*, an important example being the ability to determine chemical speciation of a wide variety of toxic elements in moist soils and biological specimens with little or no chemical pretreatment and low detection limits
• microXAFS allows one to quantify oxidation state ratios in heterogeneous earth materials and individual mineral grains. Understanding of toxicity, mobility, and containment of contaminating metals in the environment, mechanisms of trace element partitioning, and paths of strategic metal enrichment in nature.

Why a Synchrotron Based X-ray Microprobe?

- **Synchrotron radiation allows the spatial resolution to be reduced down to the micrometer level.**
  - Synchrotron radiation is several orders more intense than x-rays from tube sources.
  - Synchrotron beam is well-collimated, so that the intensity remains high at considerable distances from the source. This means that simple apertures and focusing mirrors can be used to produce small, intense beams.
  - Synchrotron radiation is highly linearly polarized which allows background from scattered radiation to be minimized by the geometry of the experiment.
- **SXRF is complementary to other microanalysis techniques**
  - electron microprobe (EMP) analysis
  - particle induced x-ray emission (PIXE)
  - laser ablation inductively coupled plasma mass spectrometry (LA-ICP-MS)
  - secondary ion mass spectrometry (SIMS).
  - SXRF is non-destructive, trace level analyses of a wide range of elements with high spatial resolution, low power deposition (X-rays deposit between 10^{-3} and 10^{-5} times less energy than charged particles).

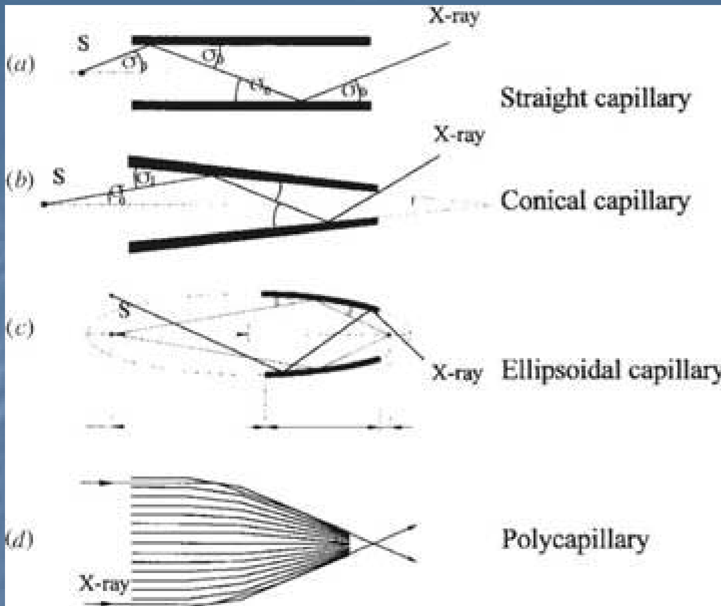

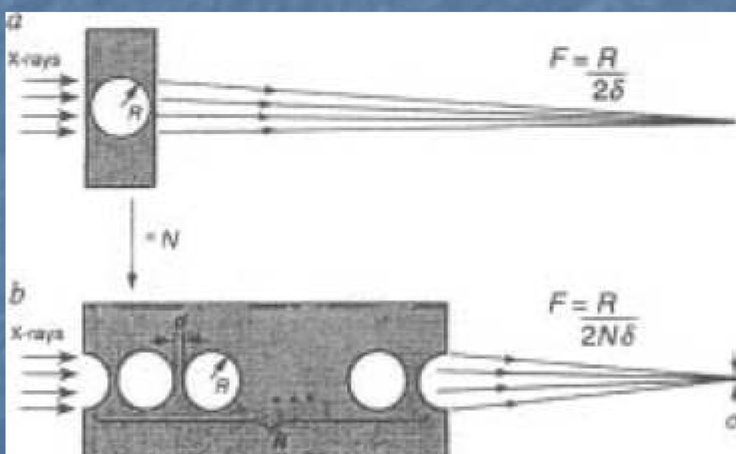

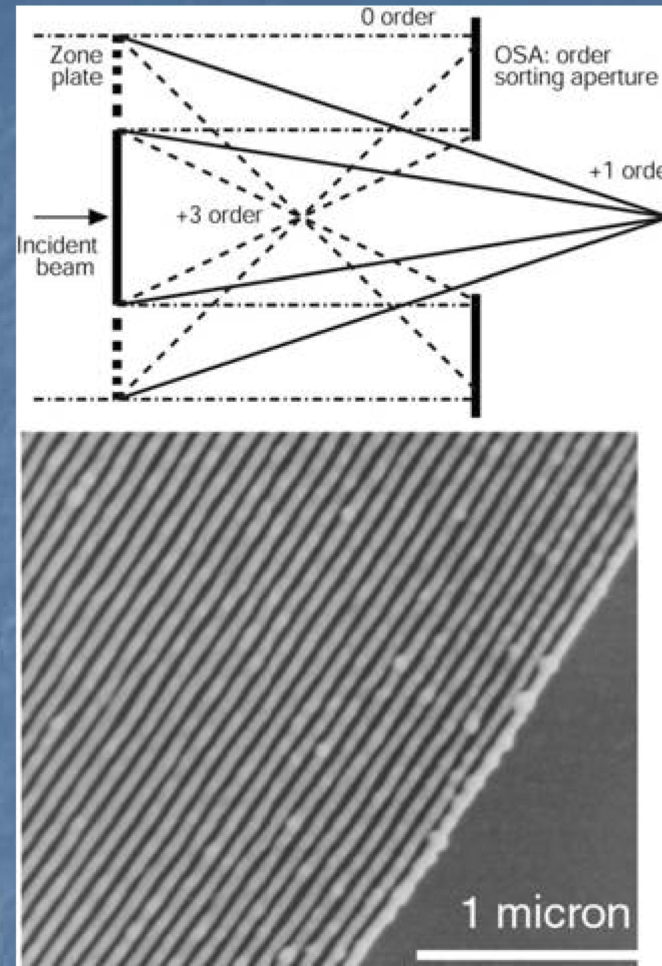

40 nm wide outermost zones in a 120 nm thick Ni zone plate

Kirkpatrick-Baez focusing mirrors

The table-top Kirkpatrick-Baez mirrors use a four-point bender and a flat, trapezoidal mirror to dynamically form an ellipsis. They can focus a 300x300 μm monochromatic beam to 10 μm a flux density gain of 10^5.

With a typical working distance of 100mm, and an energy-independent focal distance and spot size, they are ideal for micro-XRF and micro-EXAFS.

We routinely use Rh-coated silicon (horizontal) and fused-silica (vertical) mirrors to produce 4x4 μm beams for XRF, XANES, and EXAFS.

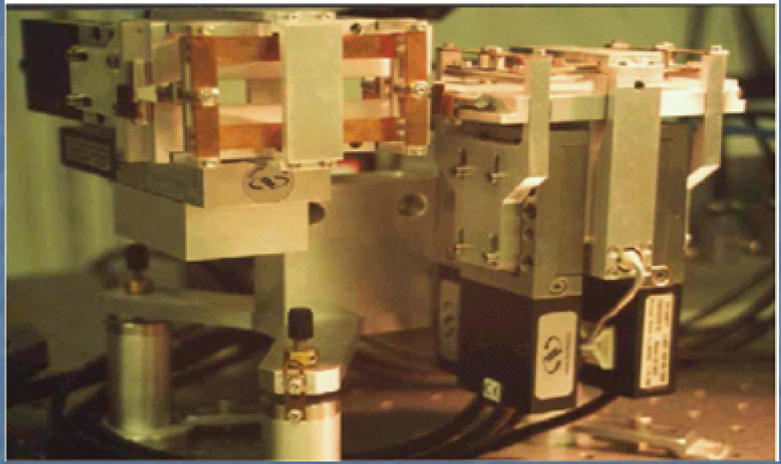

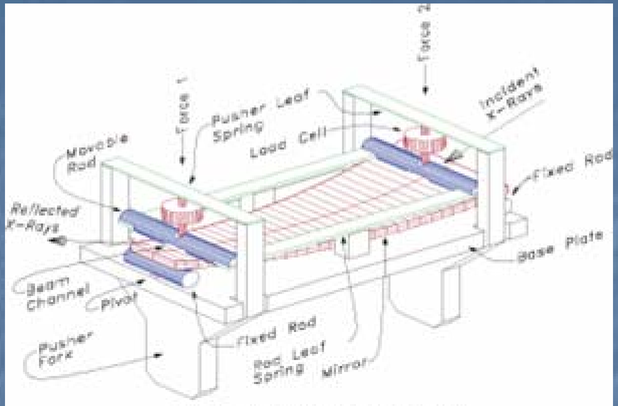

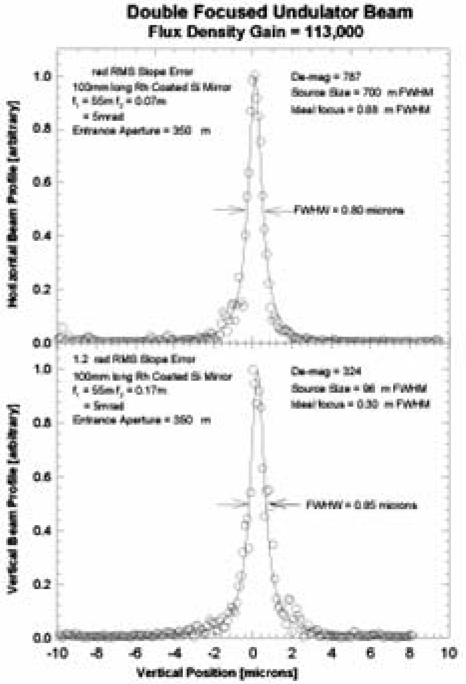

Monochromator

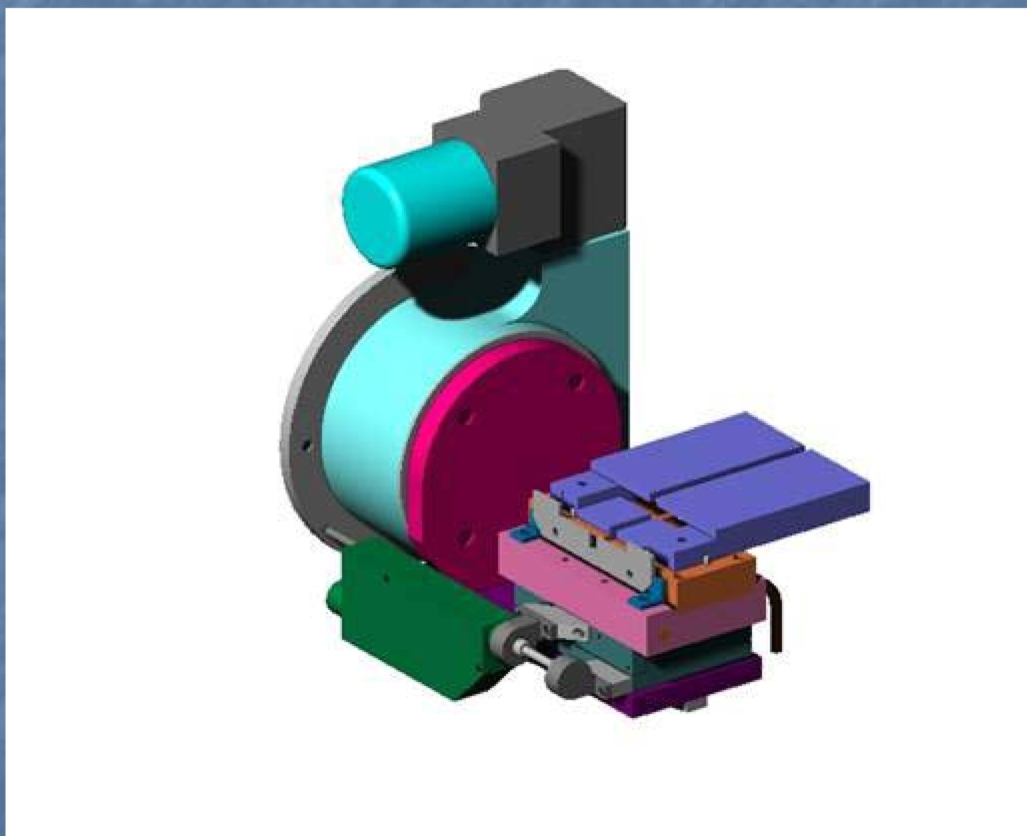

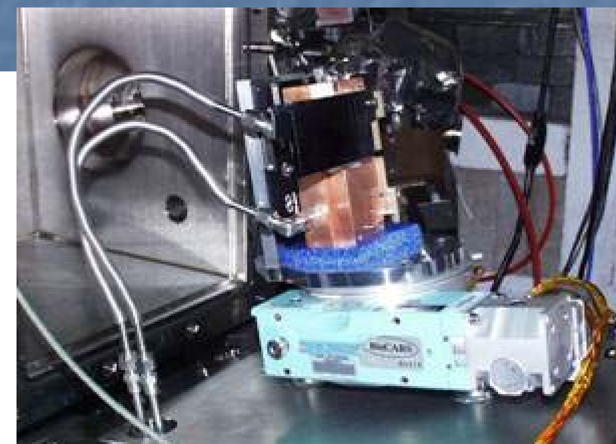

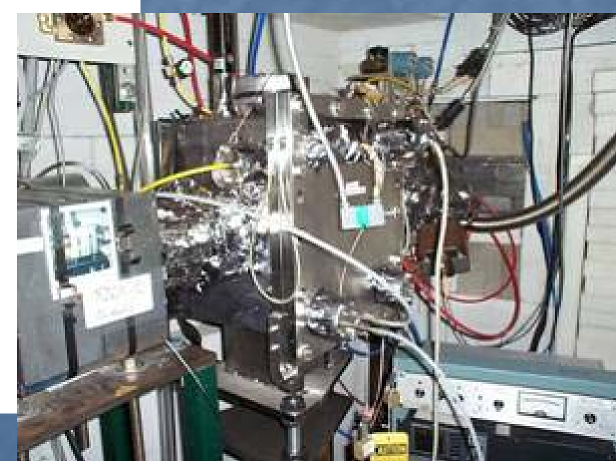

Several types of x-ray detectors are in use:

- A Canberra SL30165 Si(Li) detector (resolution about 150 eV at Mn Ka).
- A MicroSpec WDX-3 curved-crystal, wavelength dispersive spectrometer (WDS) with 4 analyzer crystals for high energy resolution detection in the 3 to 17 keV range.
- A Canberra 790-7S 9-element LEGe hard x-ray advanced array detector. The system employs digital signal processing using XIA’s DXP digital spectrometers.
- Bruker SMART 1500 CCD diffractometer, optimized for collection of data out to high 2 theta angles and on very weakly diffracting samples.
- Custom made mini ion-chambers and pin diode detectors for transmission x-ray detection.

Fluorescence Detectors

- Energy Dispersive Arrays
- Wavelength spectrometer
- Lytle chamber
- Bent Laue analyzers
- High resolution bent crystals

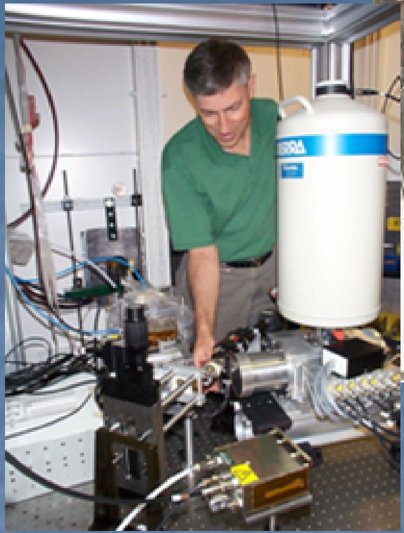

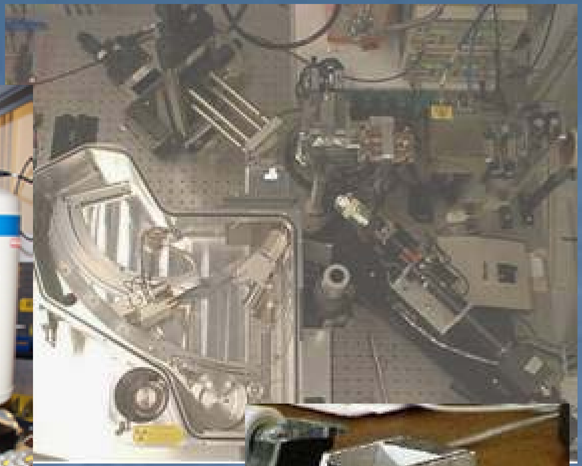

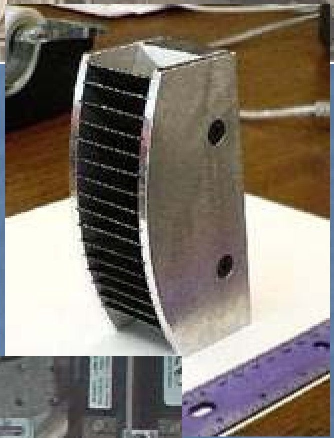

Transmission Detectors

- Ion chambers (conventional and split)

Diffraction Detectors

- CCD x-ray and optical
- Online image plate readers
- Scintillation counters

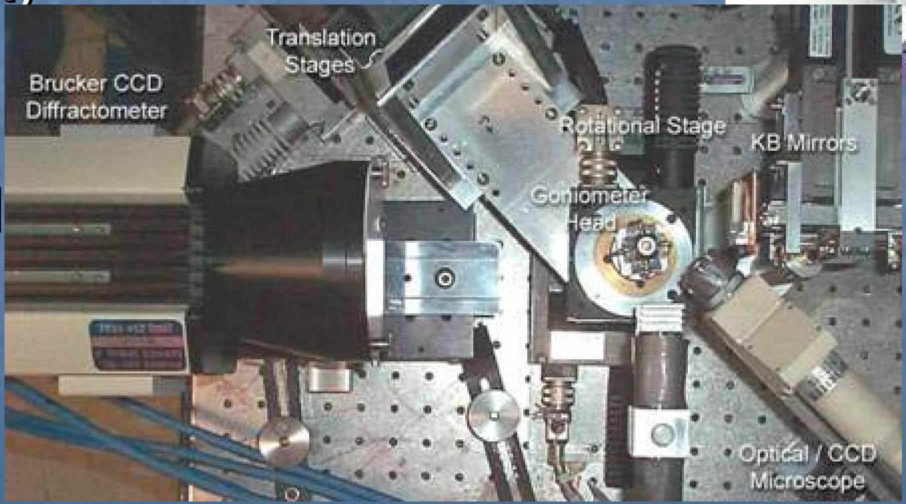

Detection Limits

- Analysis restricted to the energy interval 3-30 keV.
- The sensitivity is poor at low energy because of absorption by the Be windows and air paths, and low photoionization cross sections.
- At high energy, the production of synchrotron radiation decreases by about 1 order of magnitude for every 10 keV. K lines from elements with atomic number between S and Cs are efficiently detected whereas heavier elements require detection of L lines.
- Detection limits for L lines are somewhat higher than those for K lines of the same energy because the fluorescence yields are smaller.
- Detection limits (ppm) are typically 0.1 to 10 ppm dependent on the element and the matrix analyzed (<1 fg).

Applications

Human Health Risks From Methyl Mercury In Fish

- National Academy of Sciences expert panel reviewed the human health risks from methyl mercury in fish.
- Specifically, they reviewed epidemiological studies on children prenatally exposed to methyl mercury in seafood.
- One study is located in the Faeroe Islands in the North Atlantic on a population where exposure to methyl mercury is from consumption of whale meat.
- A second study is located in the Seychelles Islands in the Indian Ocean where methyl mercury comes from consumption of ocean fish.

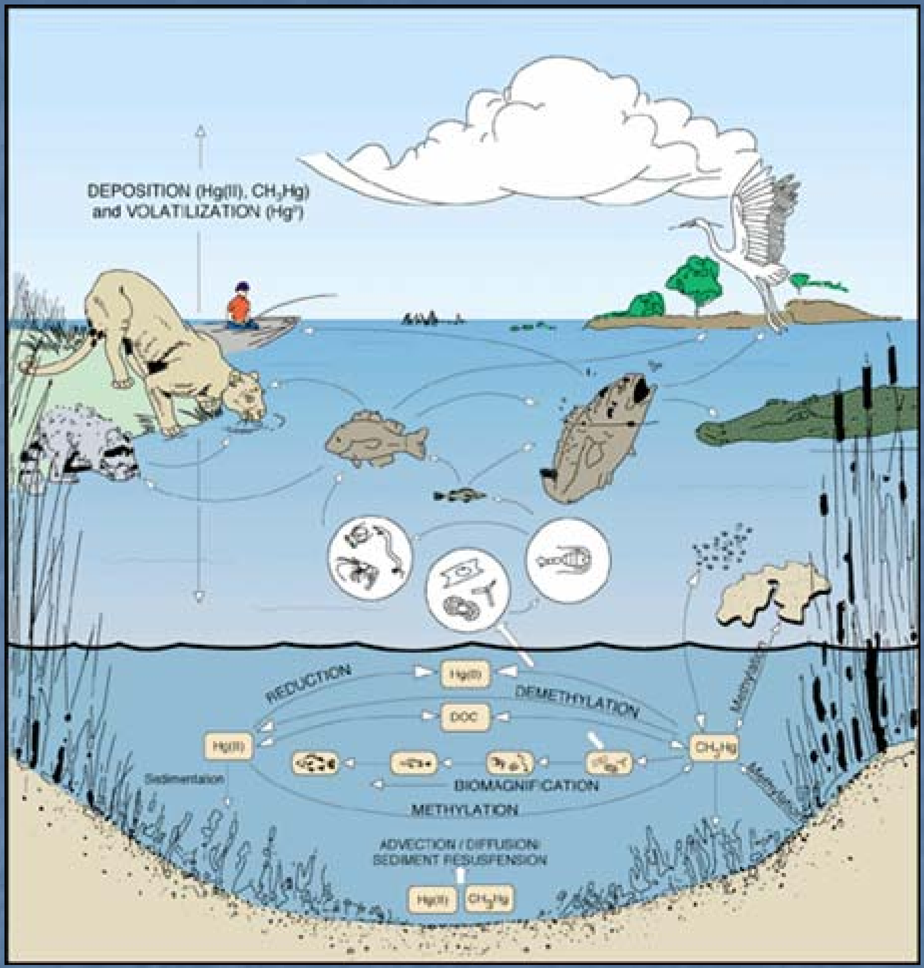

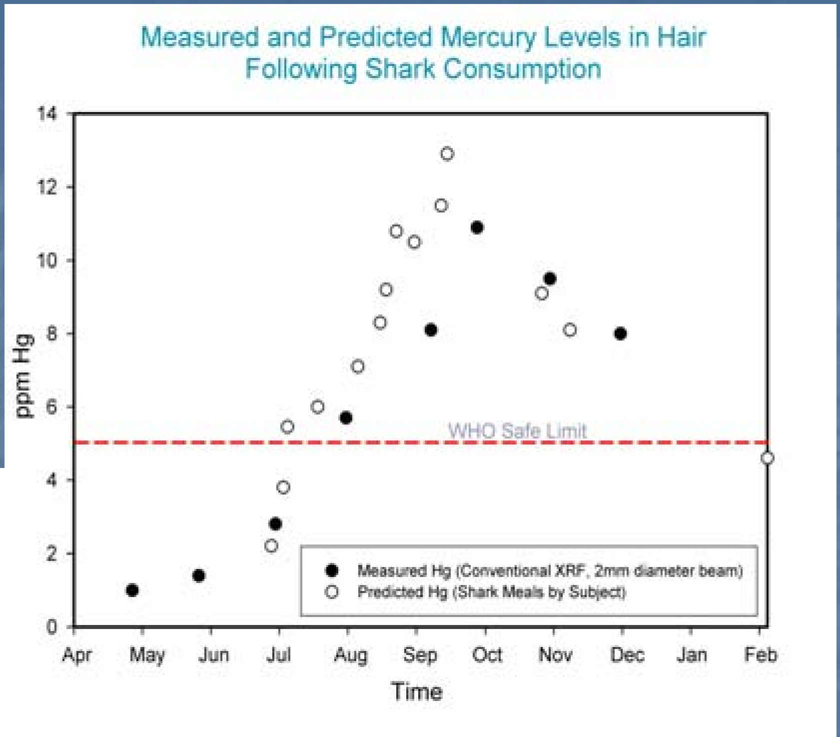
Measured and Predicted Mercury Levels in Hair
Following Shark Consumption
ppm Hg
WHO Safe Limit
Measured Hg (Conventional XRF, 2mm diameter beam)
Predicted Hg (Shark Meals by Subject)
Apr May Jun Jul Aug Sep Oct Nov Dec Jan Feb
Time
0 2 4 6 8 10 12 14

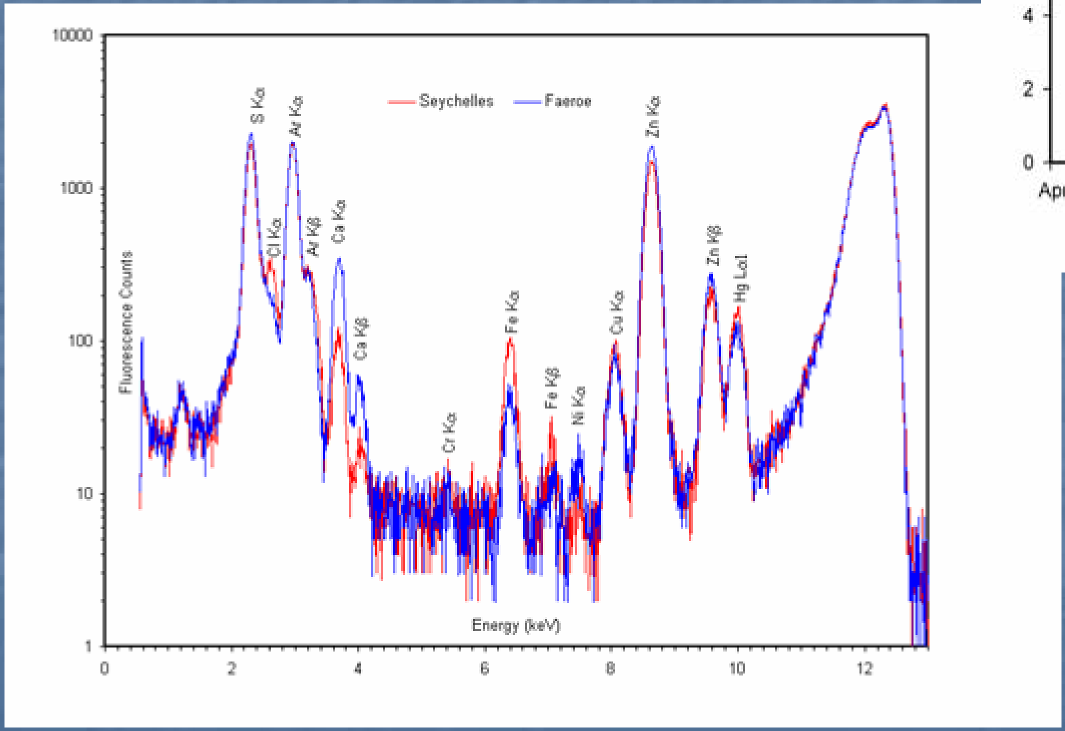
Seychelles
Faeroe
Fluorescence Counts
Energy (keV)
S Kα
Cl Kα
Ar Kα
Ar Kβ
Ca Kα
Ca Kβ
Cr Kα
Fe Kα
Fe Kβ
Ni Kα
Cu Kα
Zn Kα
Zn Kβ
Hg Lα1
1 10 100 1000 10000
0 2 4 6 8 10 12

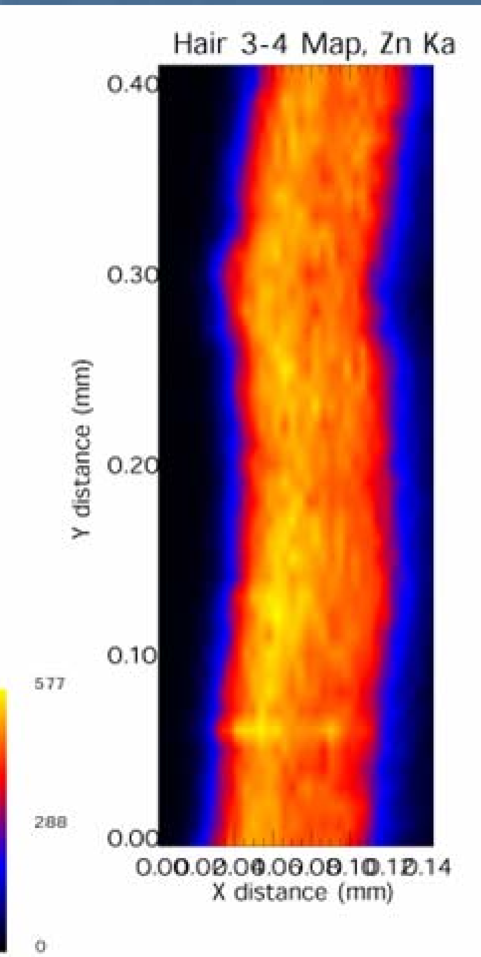
Hair 3-4 Map, Zn Ka
0.40
0.30
0.20
0.10
0.00
Y distance (mm)
0.00 0.02 0.04 0.06 0.08 0.10 0.12 0.14
X distance (mm)
577
288
0

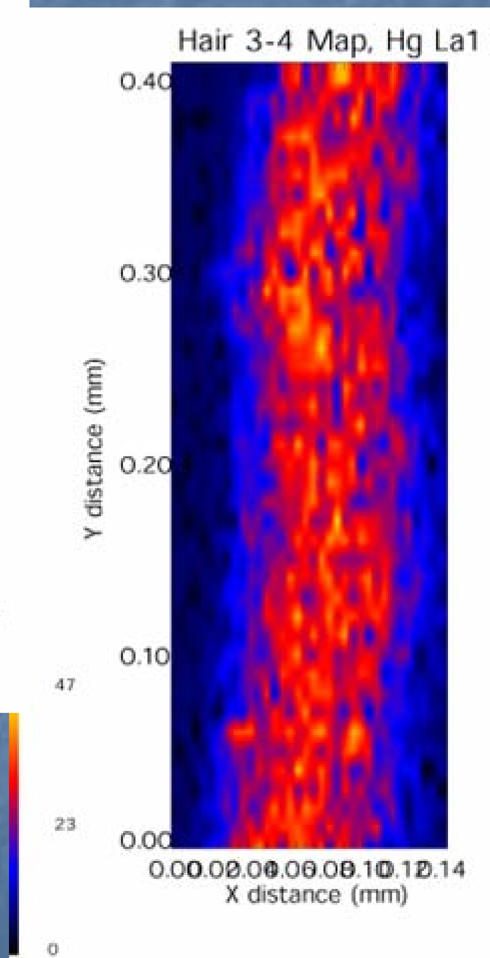
Hair 3-4 Map, Hg La1
0.40
0.30
0.20
0.10
0.00
Y distance (mm)
0.00 0.02 0.04 0.06 0.08 0.10 0.12 0.14
X distance (mm)
47
23
0

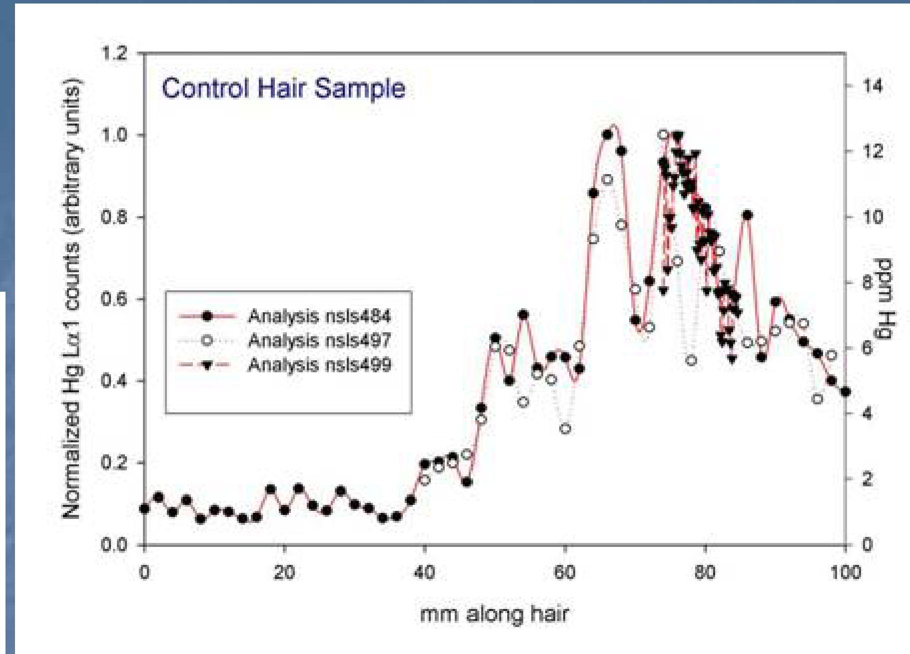
Control Hair Sample
Normalized Hg Lα1 counts (arbitrary units)
ppm Hg
mm along hair
Analysis nsls484
Analysis nsls497
Analysis nsls499
0.0 0.2 0.4 0.6 0.8 1.0 1.2
0 2 4 6 8 10 12 14
0 20 40 60 80 100

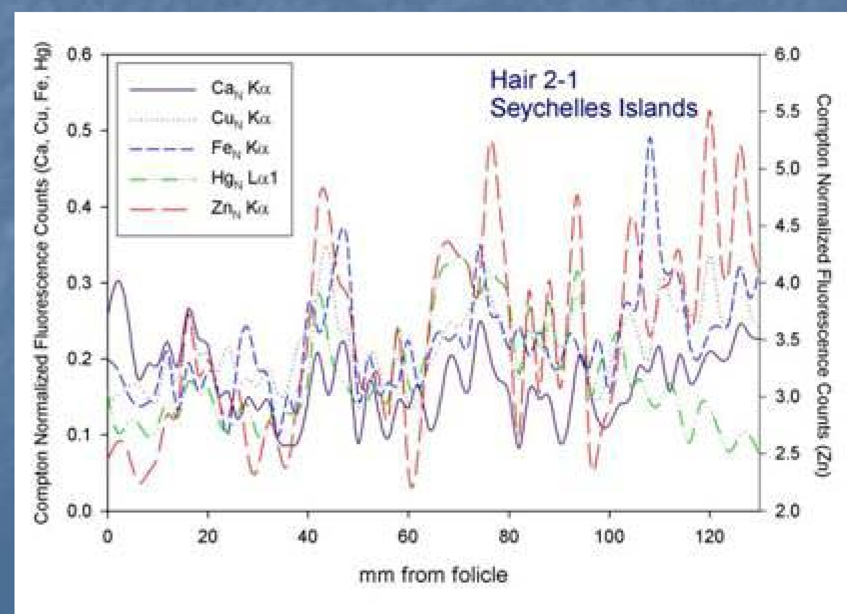
Hair 2-1
Seychelles Islands
Ca_N Kα
Cu_N Kα
Fe_N Kα
Hg_N Lα1
Zn_N Kα
Compton Normalized Fluorescence Counts (Ca, Cu, Fe, Hg)
Compton Normalized Fluorescence Counts (Zn)
mm from folicle
0.0 0.1 0.2 0.3 0.4 0.5 0.6
2.0 2.5 3.0 3.5 4.0 4.5 5.0 5.5 6.0
0 20 40 60 80 100 120

Zinc Distribution in Brain Tissue and Implications to Memory and Learning

- Zn is an essential trace element in living organisms and the adverse effects of Zn deprivation have been studied extensively
- abnormally high levels of Zn may cause learning disabilities
- Sprague-Dawley rats were exposed to controlled levels of Zn and Cu at below EPA drinking water standards
- Exposed versus control animals tested positive for spatial learning deficits using the Morris Water maze and for a decreased ability for recognition of new objects
- enhanced levels of Zn were present in the hippocampus and amygdala, which are areas of the brain linked to learning and memory

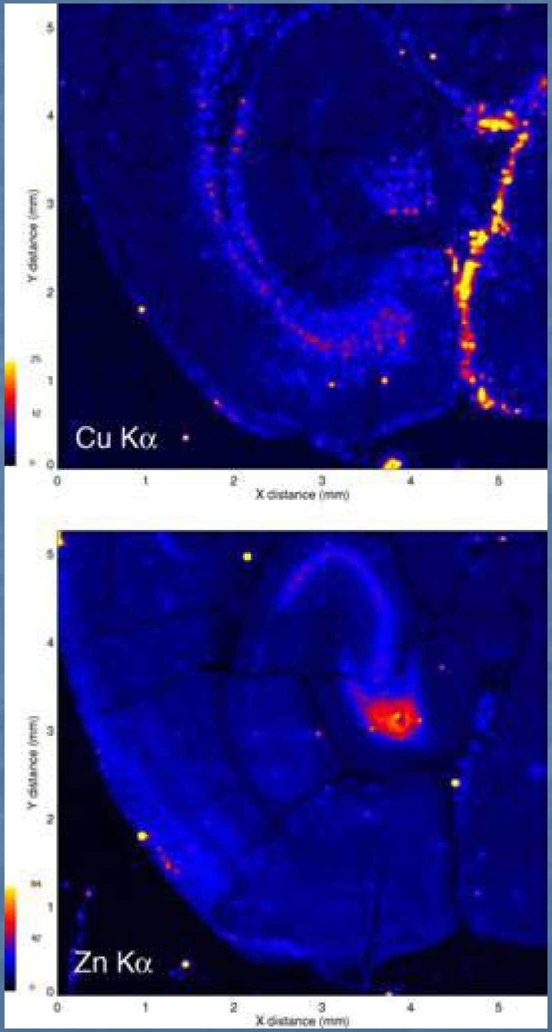

Flinn, Jones, Lanzirotti, Hunter

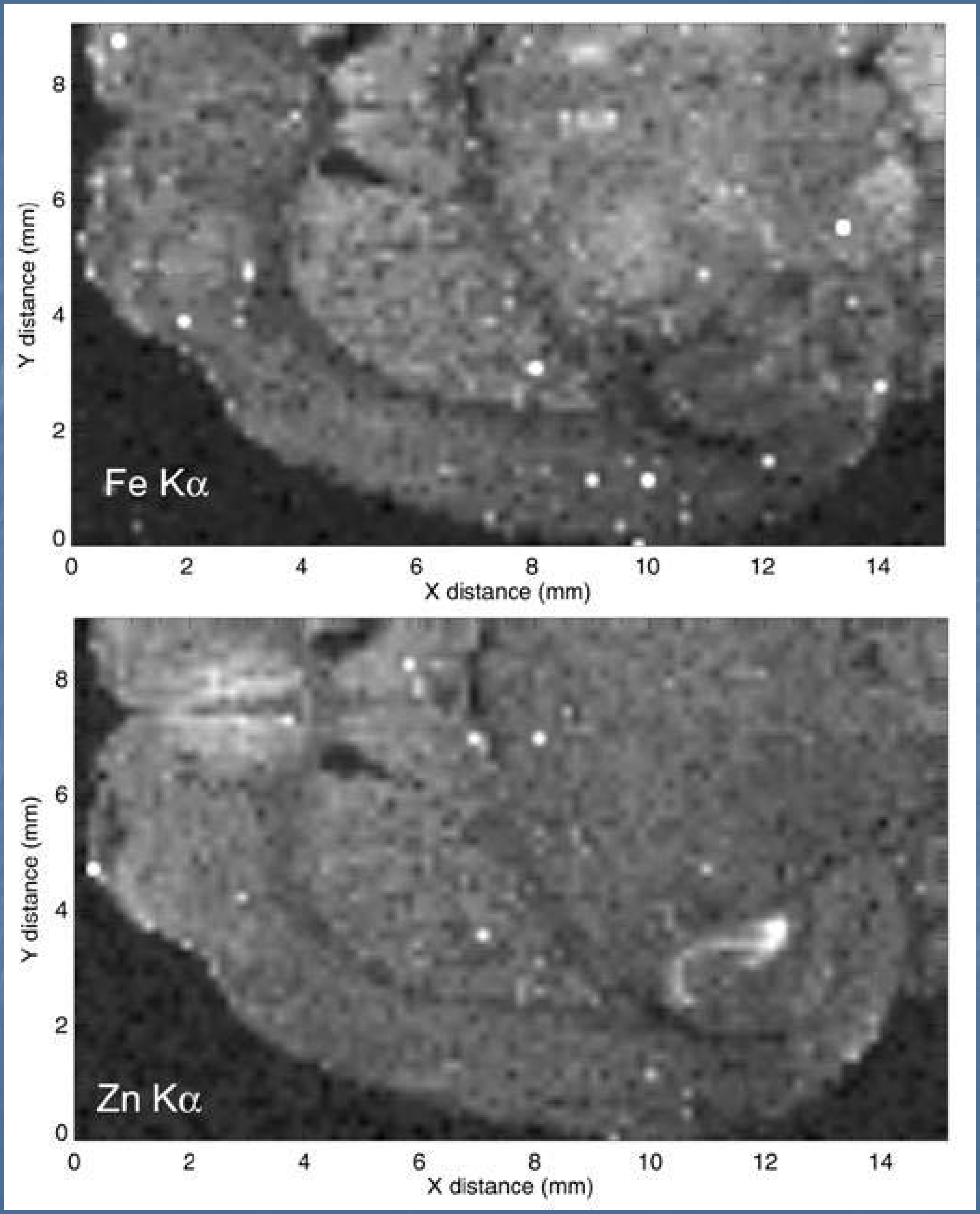

Fe Kα
Y distance (mm)
X distance (mm)
0
2
4
6
8
10
12
14
Zn Kα
Y distance (mm)
X distance (mm)

Trace Element Uptake in Plants

Lead in *N. tabacum*
Distribution in roots and stems showing effect of EDTA addition to soil

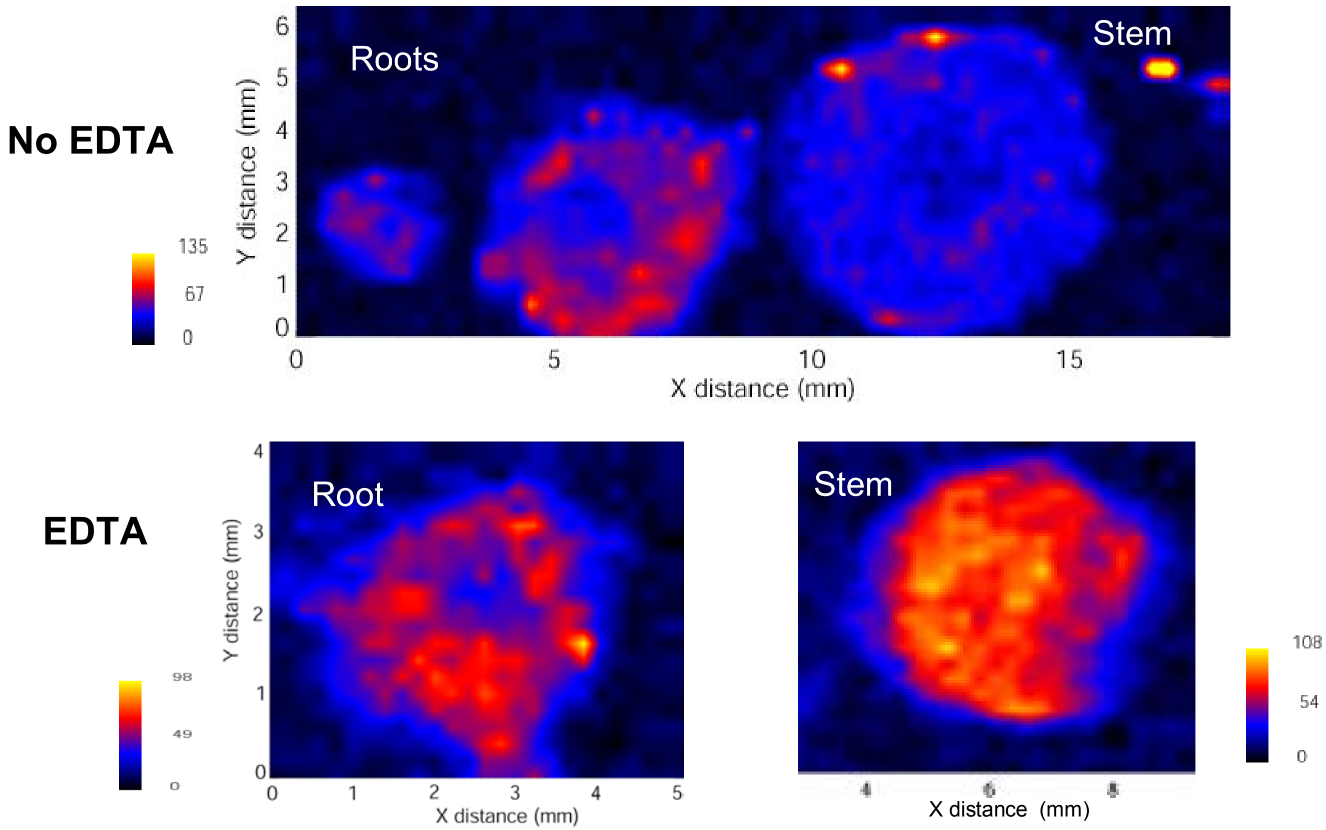

Fuhrman

Dendroanalysis

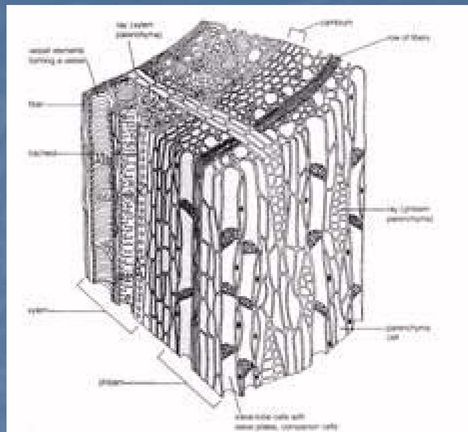

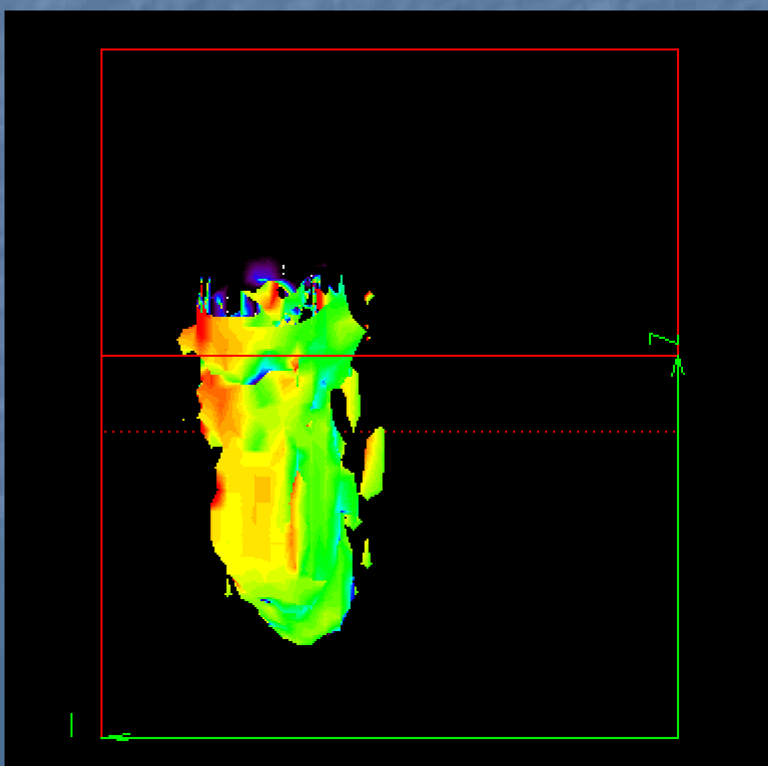

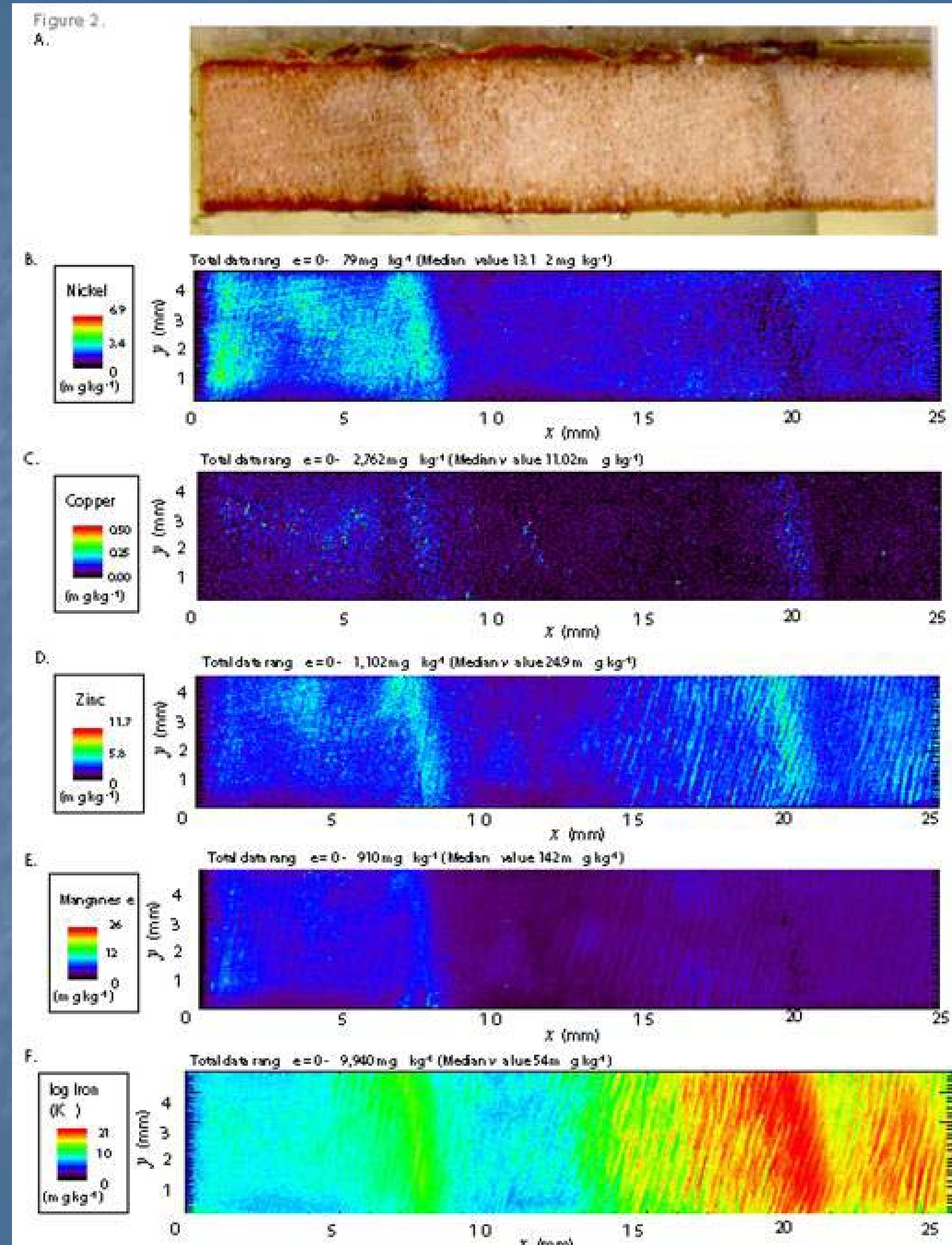

Phosphatic Fossils

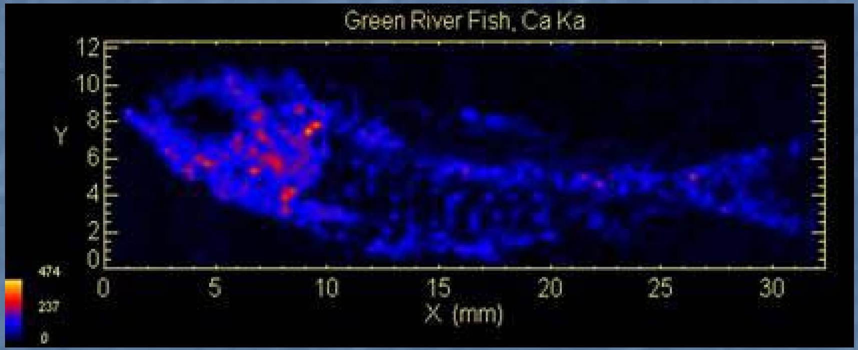

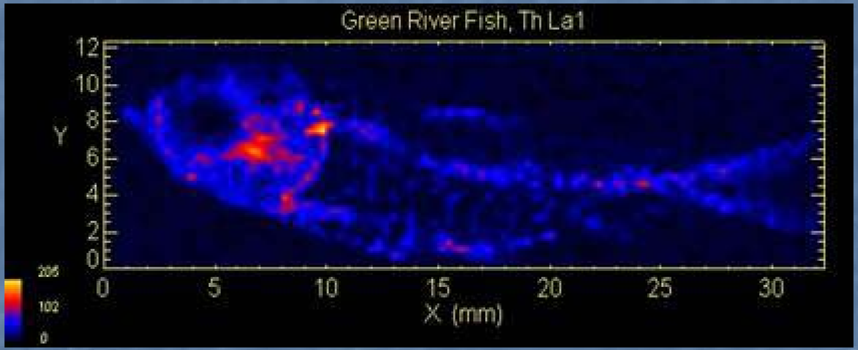

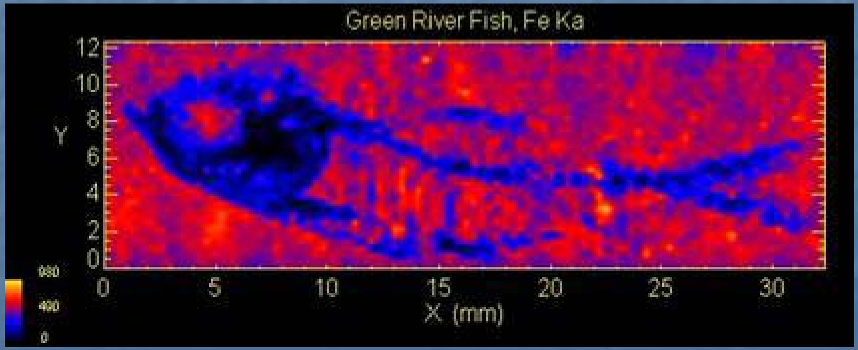

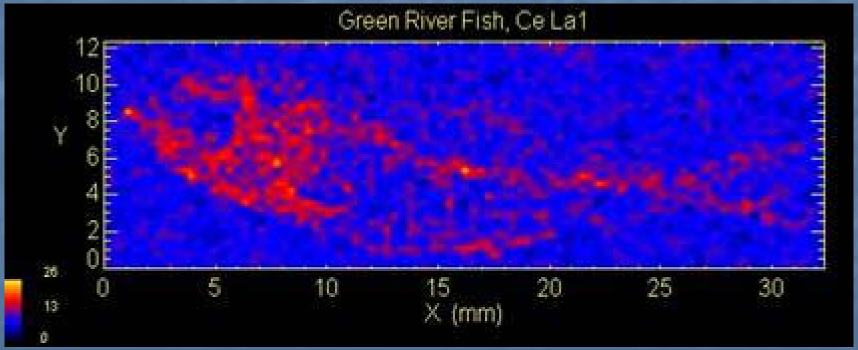

Rasbury, Cole, McCall, Lanzirotti

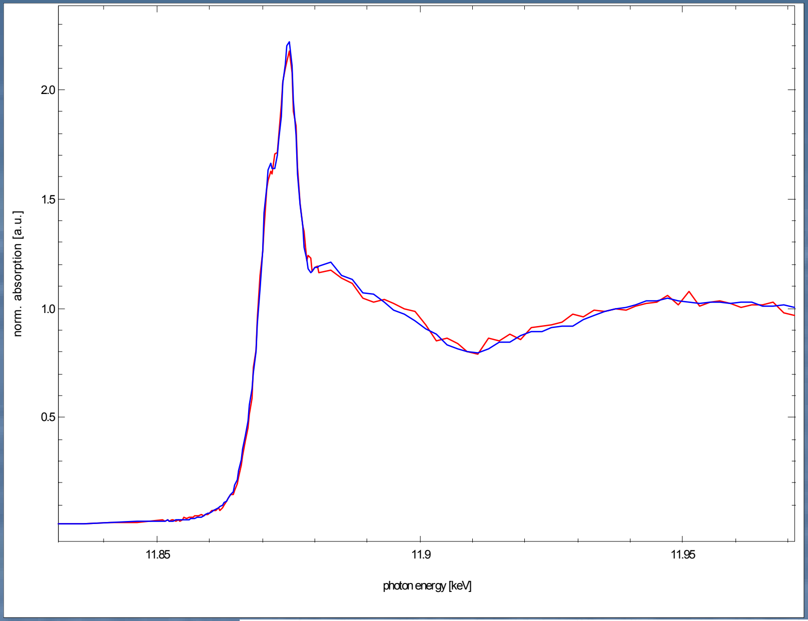

norm. absorption [a.u.]
photon energy [keV]
2.0
1.5
1.0
0.5
11.85
11.9
11.95

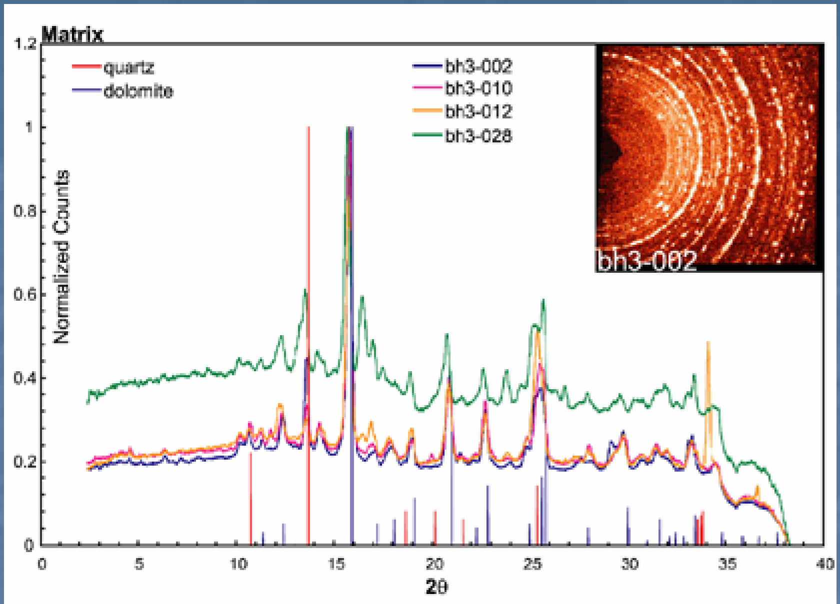

Matrix
quartz
dolomite
bh3-002
bh3-010
bh3-012
bh3-028
bh3-002
Normalized Counts
2θ

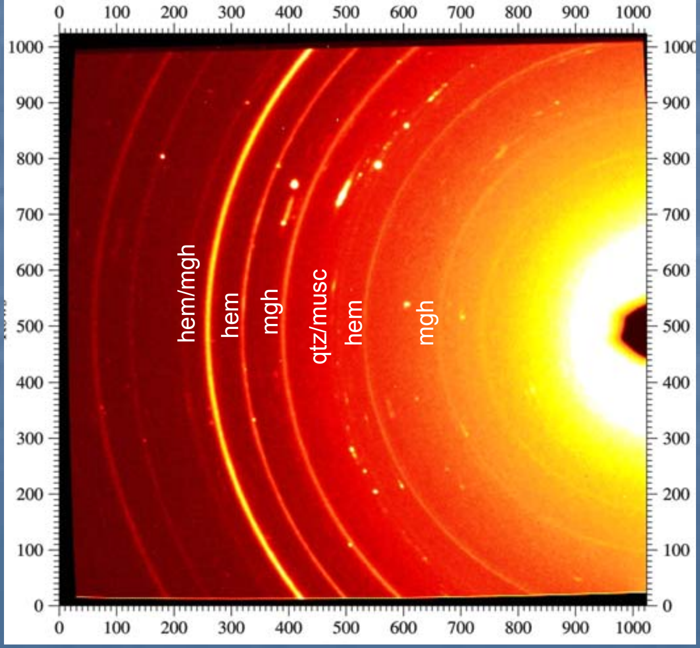

hem/mgh
hem
mgh
qtz/musc
hem
mgh

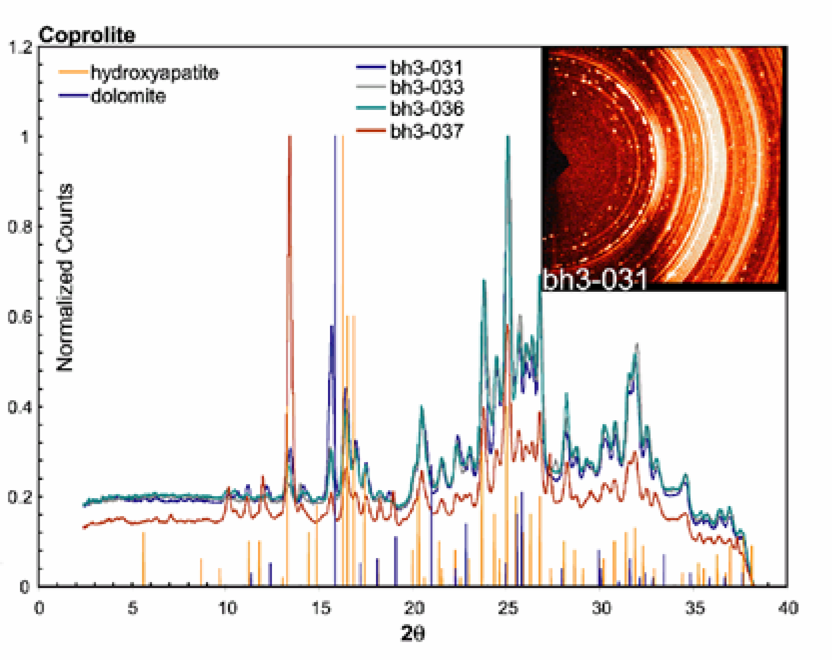

Coprolite
hydroxyapatite
dolomite
bh3-031
bh3-033
bh3-036
bh3-037
bh3-031
Normalized Counts
2θ

GSECARS 13-ID at the APS

Two Mirror-based X-ray Microprobes

Beam Line	Managing Agent(s)	Source	Beam Size (μm)	Flux @ 10 keV (ph/s)
NSLS X26A	Univ. of Chicago Univ. of Georgia Brookhaven Nat. Lab.	Bending Magnet (2.8 GeV)	10	2×10^8
APS 13-ID	GeoSoilEnviroCARS Univ. of Chicago	Undulator (7 GeV)	1	4×10^{11}

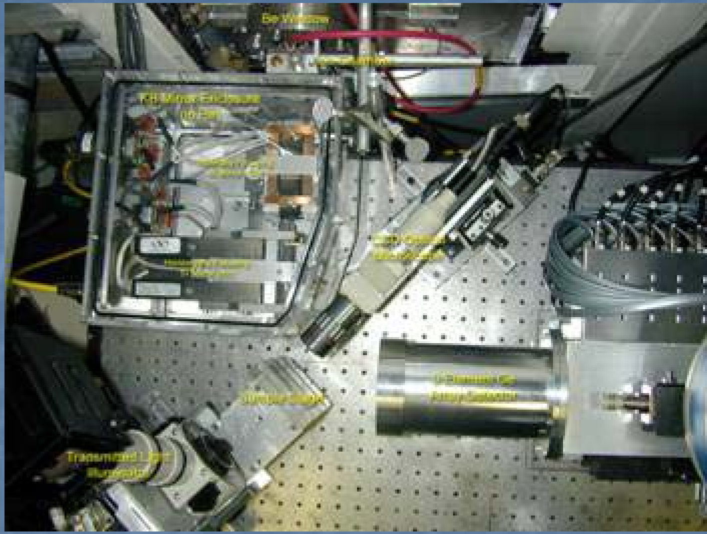

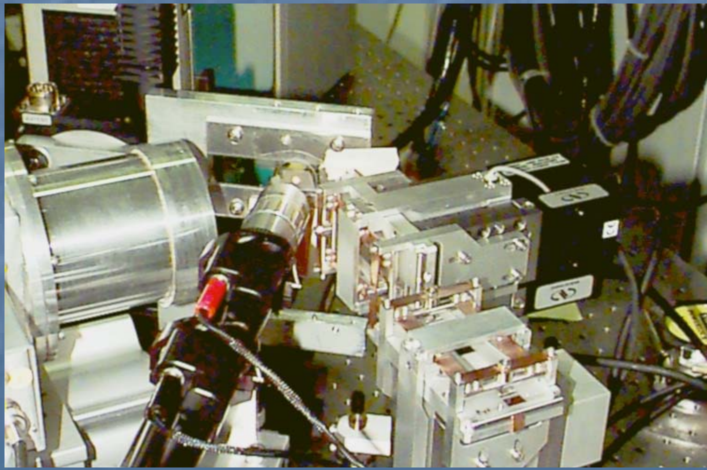

Performance

	X26A (NSLS)	Sector 13 (APS)
MicroXRF	1 ppm	100 ppb
MicroXANES	10-100 ppm	1-10 ppm
MicroEXAFS	1000 ppm – 1%	100-1000 ppm
Fluorescence Tomography	100-1000 ppm	1-100 ppm

KB Mirror Predicted Performance

		NSLS X-ray	APS (UA)	NSLS-II
Source size (vertical)	σ (μm)	27	15	4
Source size (horizontal)	σ (μm)	370	240	55
Source-mirror distance	meters	9	55	30
Sample-vert. mirror distance	meters	0.2	0.2	0.2
Sample-horiz. mirror distance	meters	0.1	0.1	0.1
Demag (vertical)		45	275	150
Demag (horizontal)		90	550	300
Deviation from ideal (vertical)*		1.2	7.4	15.0
Deviation from ideal (horizontal)*		1.0	1.1	1.5
Spot size (vertical)	FWHM (μm)	1.7	0.9	0.9
Spot size (horizontal)	FWHM (μm)	9.7	1.1	0.6

* assuming 1 microrad slope error mirrors (currently available)

Speciation Imaging using MicroXAFS

- 2D and 3D images of speciation microdistribution can be produced by collecting microXAFS spectra at each pixel
- In practice, these applications are limited by data intensiveness
- A variant used is to collect abridged spectra at each pixel; particularly useful for oxidation state mapping.

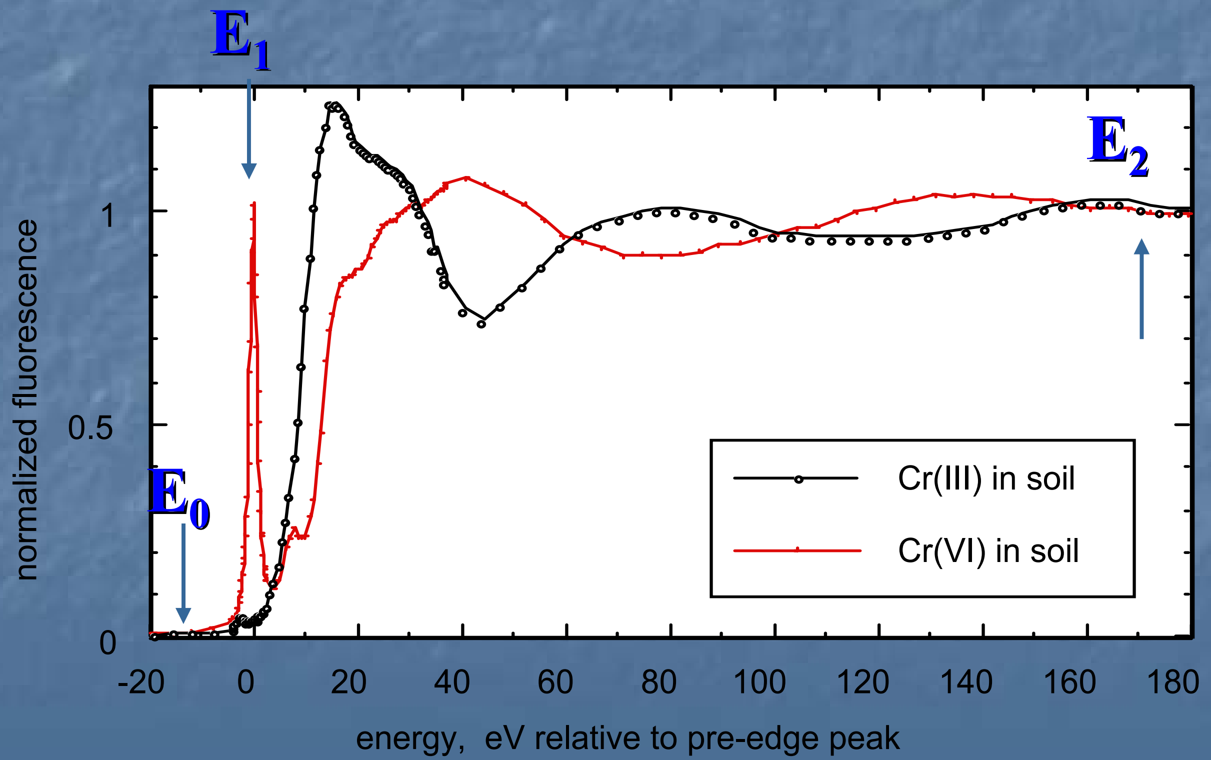

2D Oxidation State Mapping

Quick estimate of U oxidation state by measuring the U L_α XRF at 3 incident energies: E_1, E_2, E_{ref}

(P. Bertsch et al.)

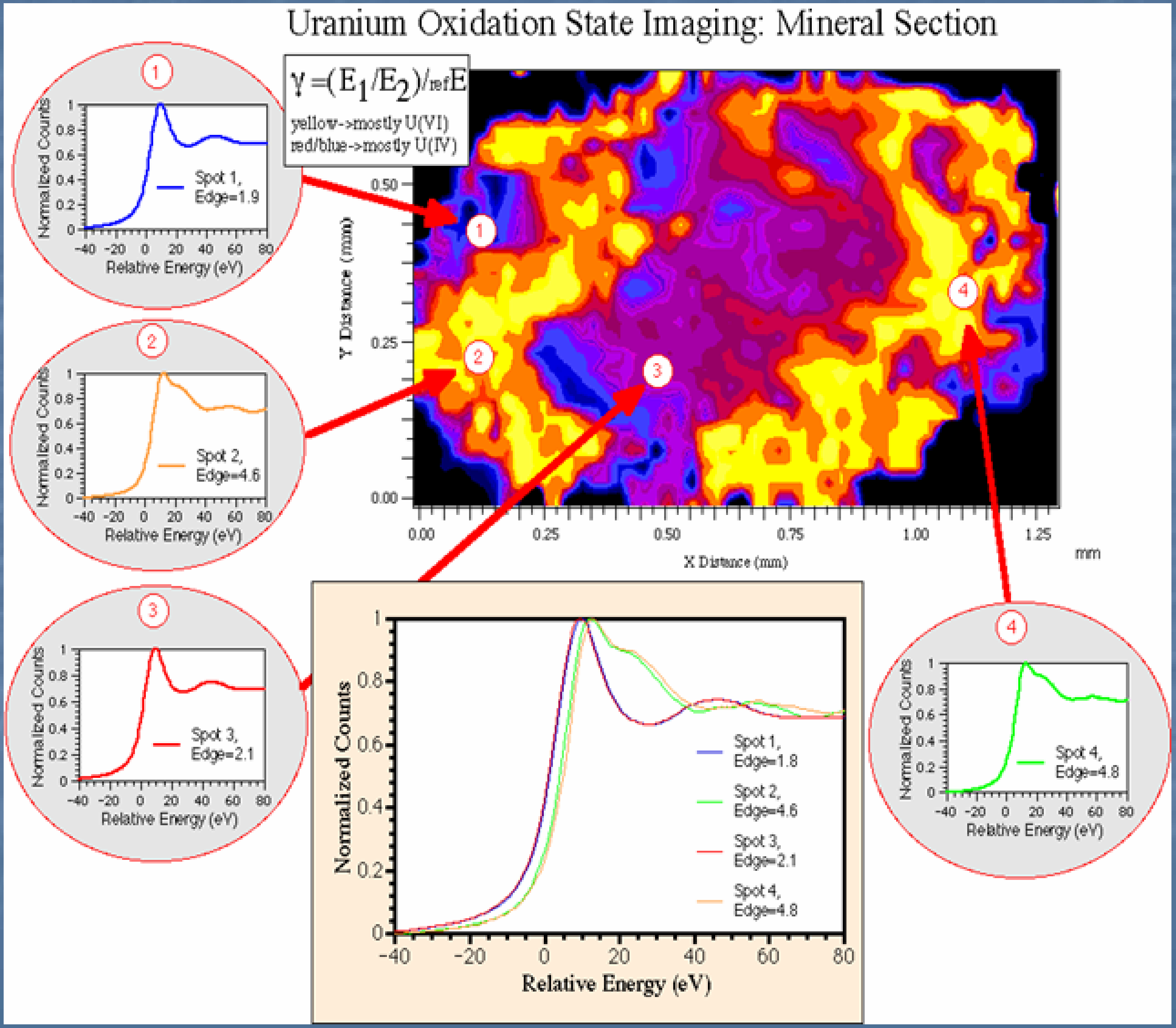

Fluorescence Microtomography

- Images of the internal distribution of specific elements
- Synchrotron XRF is very sensitive, sub-ppm
- Valuable when object cannot be sectioned at required resolution
- Absorption must not be too large
- First generation (pencil beam)
  - Requires NX translations and NR rotations for each slice.
  - Slow – but similar to conventional 2-D map
- APS Undulator Source
  - Less than 1mm vertical by 3mm horizontal
  - 1000 times more intense monochromatic beam than bending magnet

Fluorescence Microtomography Apparatus

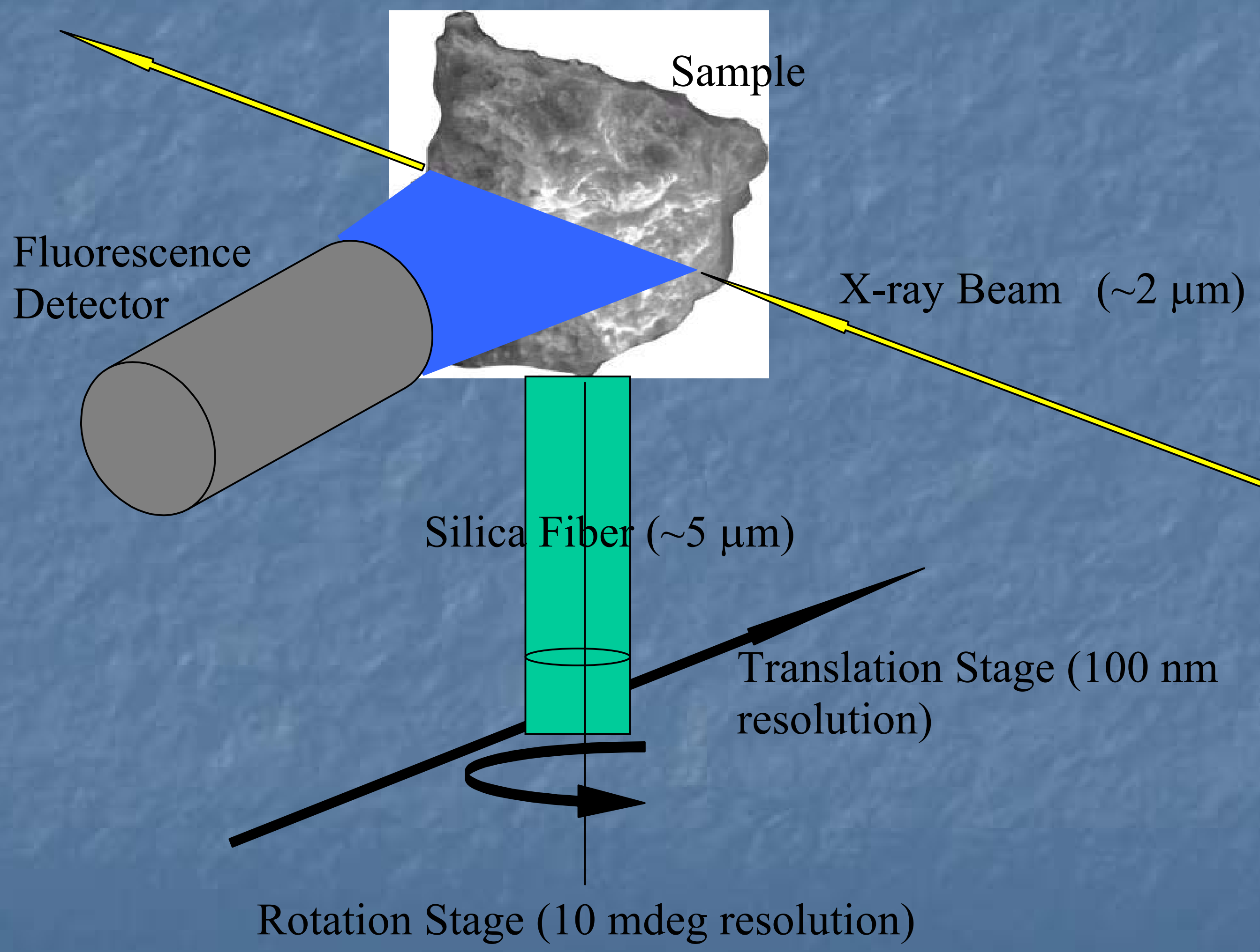

Arsenic Sequestration by Cattail Roots

N. Keon (MIT) and D. Brabander (UMass)

- Superfund site (Wells G+H wetland; *A Civil Action):* a reservoir of ~10 tons of arsenic within the upper 50 cm of the sediment profile.
- Metabolic activity of the wetland plants may be largely responsible for the sequestration of arsenic in the wetland.
- Tomograms show very strong As/Fe correlation in the ~ 40 μm plaque.

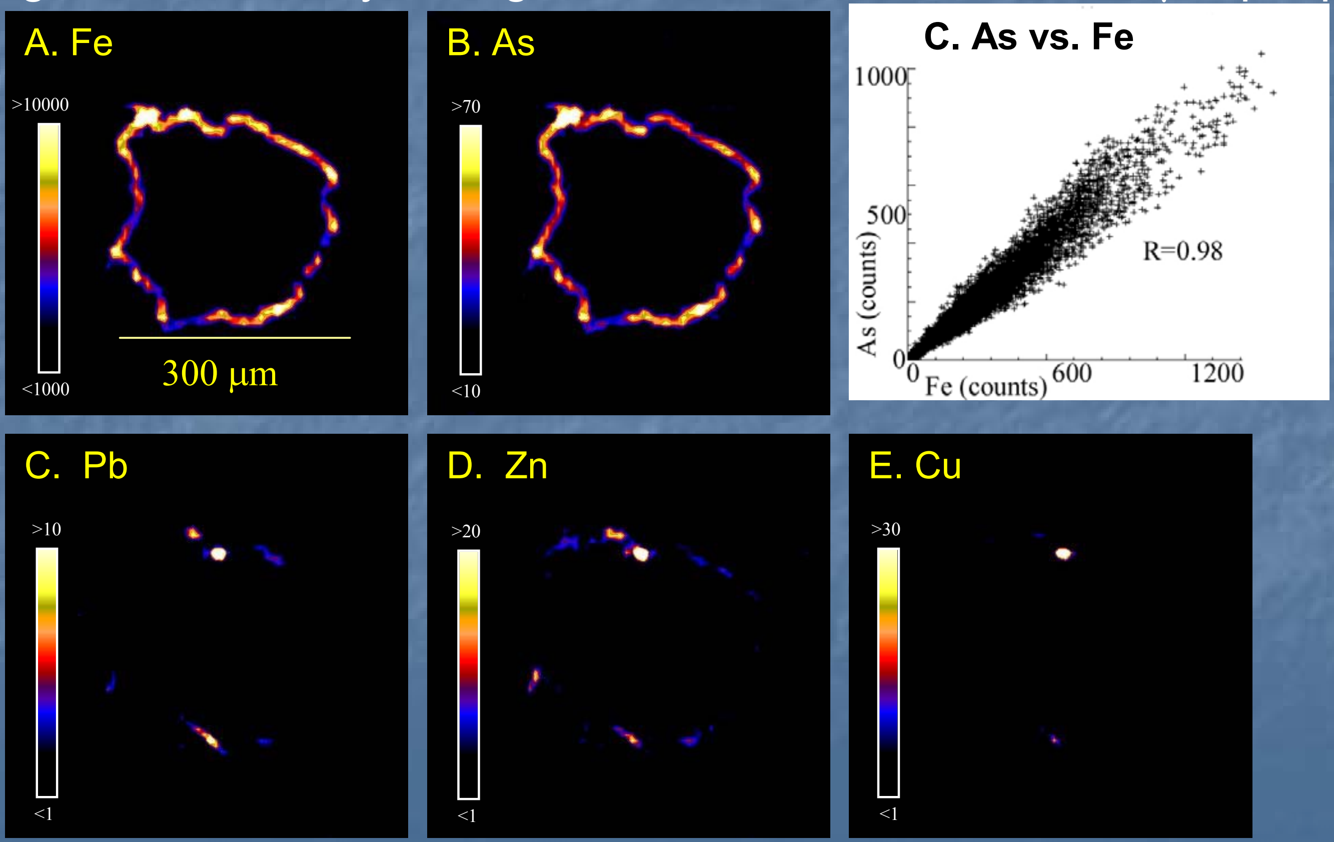

Arsenic Oxidation State Tomography

Root As K MicroXANES

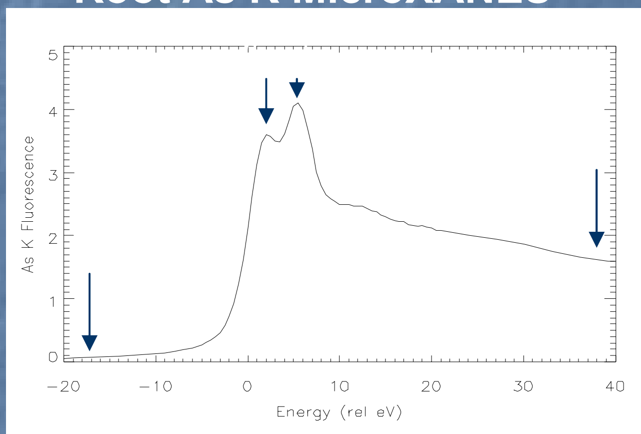

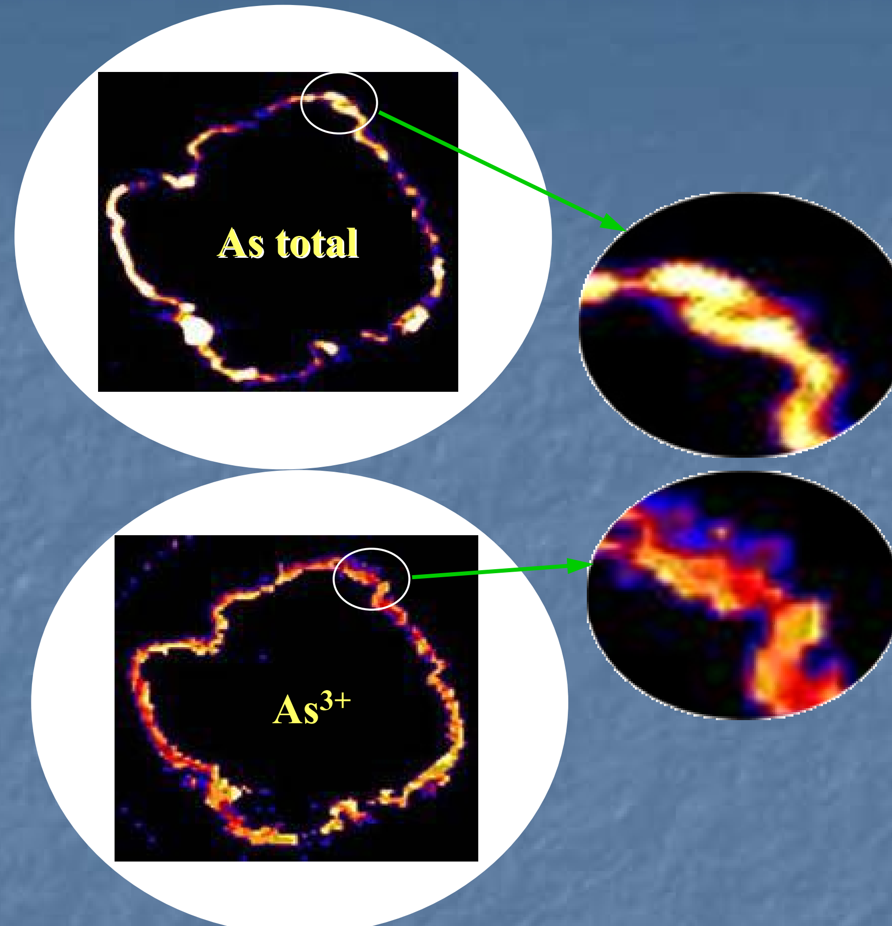

- Oxidation state tomograms show higher As^{3+}/As^{5+} ratios (more reduced arsenic) in more mature roots and a slight tendency for As^{3+} to occur on the interior of the iron-rich plaque.
- Both oxidation states of As effectively sequestered.
- Mass balance calculations suggest this sequestration has effectively reduced the As content in ground water ~100-fold.

Nickel Distribution in Hyperaccumulating Alyssum Plants (D. Sparks et al. U. Delaware)

Stem

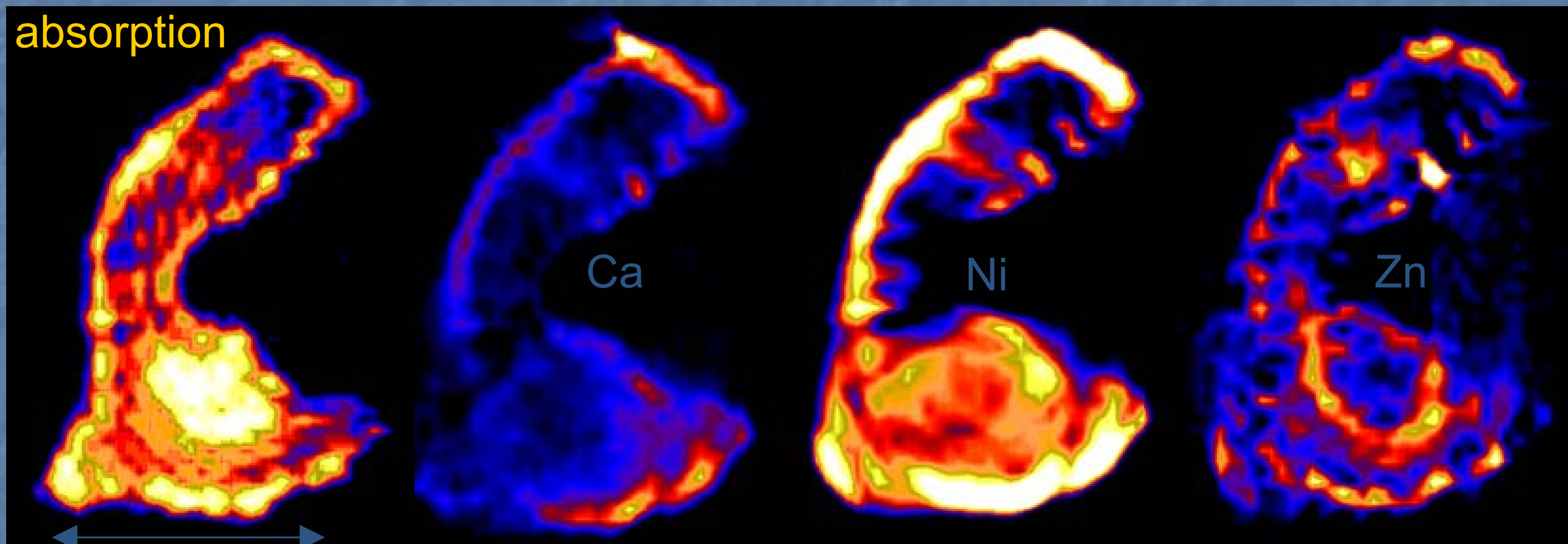

150 microns

Leaf

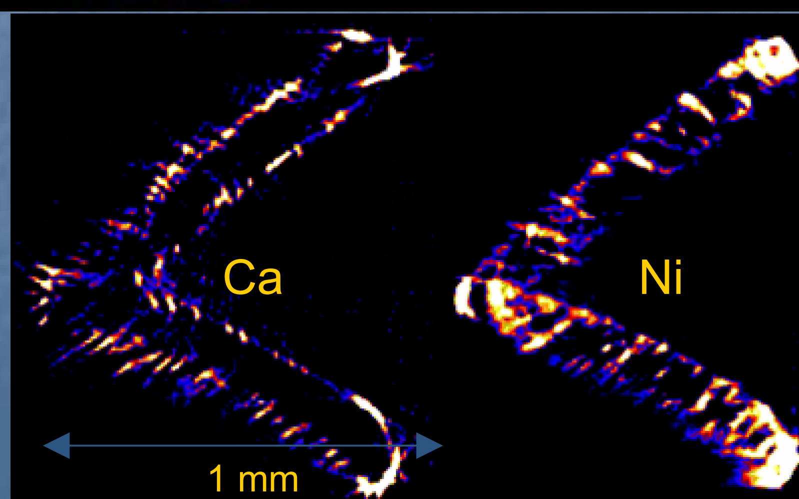

Future Directions

Increased data acquisition speed for fluorescence tomography

- Currently limited by array detector readout overhead
- DSPs have buffering capability

General purpose microprobe instrument

- Permanent installation of various detectors
- Helium enclosure for light element work
- Laser interferometer for positioning stability

Insertion device source operating over a broad energy range, esp. down to ~ 2 keV, for simultaneous work on light and heavy elements

- APS undulator A limited on low end to ~ 3 keV